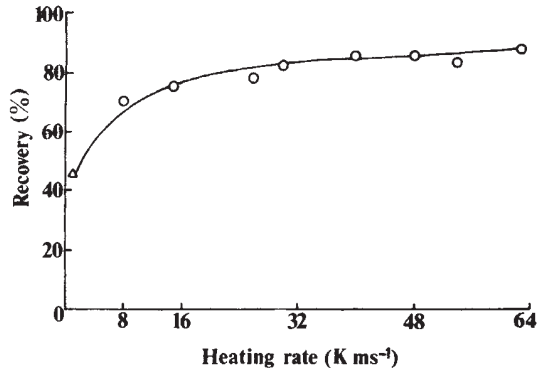

Fig. 2 Recoveries of Cd as a function of heating rate from an aqueous solution containing NaCl 1.0×10^{-8} kg + $MgCl_2$ 1.2×10^{-9} kg + $CaCl_2$ 4.0×10^{-10} kg as a function of the heating rate. Cd λ 228.8 nm. Cd = 4.0×10^{-14} kg. Atomization temperature, 1,900 K.

temperature of 2,200 K (same as that of Fig. 1*a*); curve *E* is for the blank containing an aqueous solution of 0.5% (wt/v) NaCl, and shows that the background absorption due to the NaCl matrix is completely absent, which is highly significant. Figure 1*b* shows that the two absorption pulses are identical in both amplitudes and areas, and the matrix effects have been completely eliminated. In Fig. 1*b* the lead signal appears much later in time (compared with Fig. 1*a*), and hence, the appearance temperature for lead is considerably higher than that in Fig. 1*a*. In Fig. 1*b* the considerably higher appearance temperature for Pb and atomization in constant temperature are crucial for eliminating chloride matrix interferences. In Fig. 1*a*, atomization of lead occurred in non-isothermal conditions at a temperature which was considerably lower than that in Fig. 1*b* and at a time when the temperature of the atomizer increased at a very rapid rate from 600 to 2,200 K; hence, the pressure inside the graphite tube changed from 1 to 3.7 atm, which resulted in partial expulsion of the lead chlorides vapour; also the extent of dissociation of lead chlorides to lead atoms was less at the lower temperature. It is concluded that the elimination of the matrix effect in Fig. 1*b* is due to atomization at a constant temperature and at a much faster rate of heating with the technique.

Figure 2 shows the recoveries of Cd from an aqueous solution of $NaCl + MgCl_2 + CaCl_2$ matrices as a function of heating rates at the isothermal atomization temperature of 1,900 K. Even at the highest heating rate used (63 K ms^{-1}), the recovery curve is seen to rise slightly, indicating a need for still higher heating rates for greater recoveries.

We conclude that even with the present laboratory-made instrumentation, the technique gives fairly accurate and precise results, which should improve with better instrumentation.

The technique with its simplified and shortened analytical procedure should save considerable time and cost per analysis. The limitation of this technique is that in the solid-sampling technique, the small sample (mg) requirement may present a sampling problem if the solid sample is inhomogeneous.

H.A.H. thanks the Government of Iraq for a postgraduate scholarship. This work was supported by grants from the Natural Sciences and Engineering Research Council of Canada.

Received 14 April; accepted 30 September 1980.

1. L'vov, B. V. *Spectrochim. Acta* **33B**, 153–193 (1978).
2. Chakrabarti, C. L. *et al. Analyt. Chem.* **52**, 167–176 (1980).
3. L'vov, B. V. *Atomic Absorption Spectrochemical Analysis*, 221 (Hilger, London, 1970).
4. Sturgeon, R. E. & Chakrabarti, C. L. *Prog. Analyt. Atom. Spectrosc.* **1**, 1–199 (1978).
5. Nakahara, T. & Chakrabarti, C. L. *Analyt. chim. Acta* **104**, 99–111 (1979).
6. Chakrabarti, C. L., Wan, C. C. & Li, W. C. *Spectrochim. Acta* **35B**, 93–105 (1980).

Forces between mica surfaces bearing layers of adsorbed polystyrene in cyclohexane

Jacob Klein

Polymer Department, Weizmann Institute of Science, Rehovot, Israel

Direct measurements of the forces acting between polymer surface phases adsorbed at interfaces have only recently been reported[1–3]. These were carried out in good solvents and showed that repulsive forces were acting between the adsorbed layers; these forces increased monotonically as the surfaces approached each other. In certain conditions, however, for example, those leading to the flocculation of sterically stabilized colloidal systems, one expects the surfaces bearing the adsorbed phases to attract before repelling each other[4,5]. I have measured the forces acting between two curved mica surfaces immersed in cyclohexane at 24 °C (a worse than θ solvent at this temperature), each bearing a surface layer of adsorbed polystyrene ($M_w = 6\times10^5$). No forces are observed at surface separations larger than about three radii of gyration of the polymer; on closer approach a strong attraction develops between the surfaces, changing to an ultimate repulsion as the surfaces approach closer than about one radius of gyration. Between times of a few minutes and several hours the forces are stable, well behaved and reproducible.

The experimental technique (Fig. 1) is an extension of that developed by Tabor *et al.*[6,7], and recently modified by Israelachvili and Adams[8], to measure (1) the forces $F(D)$ acting between two curved mica surfaces a distance D apart; (2) the mean refractive index $n(D)$ of the medium separating the surfaces.

$F(D)$ was first determined between the mica surfaces in pure cyclohexane; polystyrene solution was then added to the cell, to a final concentration of $7\pm2\times10^{-6}$ g ml^{-1}. After 10 h incubation in the polymer solution, $F(D)$ was measured both in compression and decompression; measurements were repeated in the solution over a period of some hours, following which the polymer solution was entirely removed (save for ~1 ml between the mica surfaces) and replaced by pure cyclohexane. The surface–surface forces were then measured at intervals of between 5 min and several hours, and at compression/decompression rates of between 20–60 min per cycle, over a period of 48 h. The temperature of all experiments was 24 ± 0.5 °C.

The results are shown in Fig. 2. No forces are observed as the surfaces approach from $D \simeq 300$ nm down to $D \simeq 60$ nm; on closer approach an attractive force arises between the surfaces, and on further decreasing D they jump from A (Fig. 2*b*) to a new stable position at B (such jumps are expected[6] whenever $\partial F/\partial D > K$, the force constant of the spring supporting the lower mica surface—see Fig. 1). Further approach results in a strong repulsion. On separation (decompression) the surfaces jump from C to a new stable position at E. The region AC is a region of instability ($\partial F/\partial D > K$) where $F(D)$ and $n(D)$ cannot be determined[8]. The 'jumps' (A → B, C → E) are not instantaneous, and up to 300 s are required for new stable positions to be established: this is interpreted as the time taken by the opposing adsorbed layers to interdiffuse (on compression) or disentangle (on decompression). The forces are stable, and within the estimated errors, reversible and reproducible over the several compression/decompression cycles. In particular, the surfaces could be held in a strongly repulsive region around $D = 14$ nm under a fixed force for up to 3 h with no resulting change in the separation.

0028–0836/80/470248—03$01.00

The refractive index $n(D)$ of the medium separating the mica surfaces varied between $n = 1.56 \pm 0.02$ at $D = 14$ nm and $n = 1.43 \pm 0.012$ for $D \geq 80$ nm (Fig. 2*c*). The values of n were determined, following incubation, in the polymer solution, and were unchanged on replacing the solution by pure solvent, and up to 48 h later. From the bulk refractive indices of cyclohexane (1.426) and polystyrene (1.595) the value of n ($D = 14$ nm) corresponds to an adsorbance on each mica surface of around 6 mg m^{-2} of polymer. This compares with equilibrium adsorbances of 3–8 mg m^{-2} for polystyrene adsorbed onto various substrates from cyclohexane at the θ temperature[9].

In the conditions of only moderately high polymer molecular weight and extremely low bulk concentration of polymer used in the present study, the polymer solution, though considerably below the Flory θ- temperature for this system (35 °C), is above its cloud-point temperature[5,10]. Thus no phase-separation occurs[10] (other than adsorption); polymer dimensions are expected to be somewhat smaller than their unperturbed value[5,11]. Because very long times may be required before an adsorbed layer reaches equilibrium, we cannot be sure that, given much longer times, the system may not undergo further change. The fact that replacing the polymer solution by essentially pure solvent does not significantly change the adsorbed layer suggests that the adsorption may behave irreversibly. The onset of interaction between the surfaces at $D \simeq 60$ nm indicates that significant overlap between the opposing polymer layers begins at this value of D, corresponding to adsorbed layers extending some 30 nm from each mica surface. This compares with an unperturbed radius of gyration $R_g = 21$ nm for this polymer[13], and with ellipsometrically[9] and viscometrically[12] measured equilibrium layer thicknesses of 40 nm for poly-

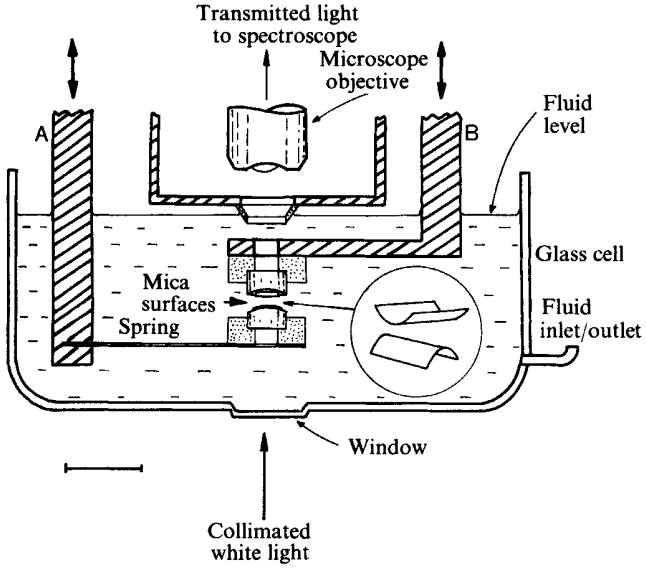

Fig. 1 Section of the apparatus used to measure forces between mica surfaces in a liquid medium. The surfaces are mounted in a crossed-cylinder configuration (inset) on cylindrical quartz lenses, within a glass cell (volume ~150 ml); their separation D is controlled (to 0.2 nm) by the rigid arms A, B, using a three-stage mechanism (two micrometers and a piezoelectric crystal) similar to that previously described[8]. The method is based on an optical technique utilizing white-light multiple-beam interferometry, which can measure both D (to 0.3 nm) and the refractive index $n(D)$ of the medium separating the surfaces, as well as their radii of curvature[6,7]. The top mica surface is directly mounted on the rigid arm B, while the bottom surface is mounted on A through a leaf spring of force constant K (75 N m^{-1}). By measuring the change in D in response to known, applied relative displacements of the rigid arms A and B, $F(D)$ may be determined[8]. The glass cell is mounted within an airtight stainless steel box, which is in turn placed on a mechanically insulated platform within a thermally insulated chamber. Scale bar, 2 cm.

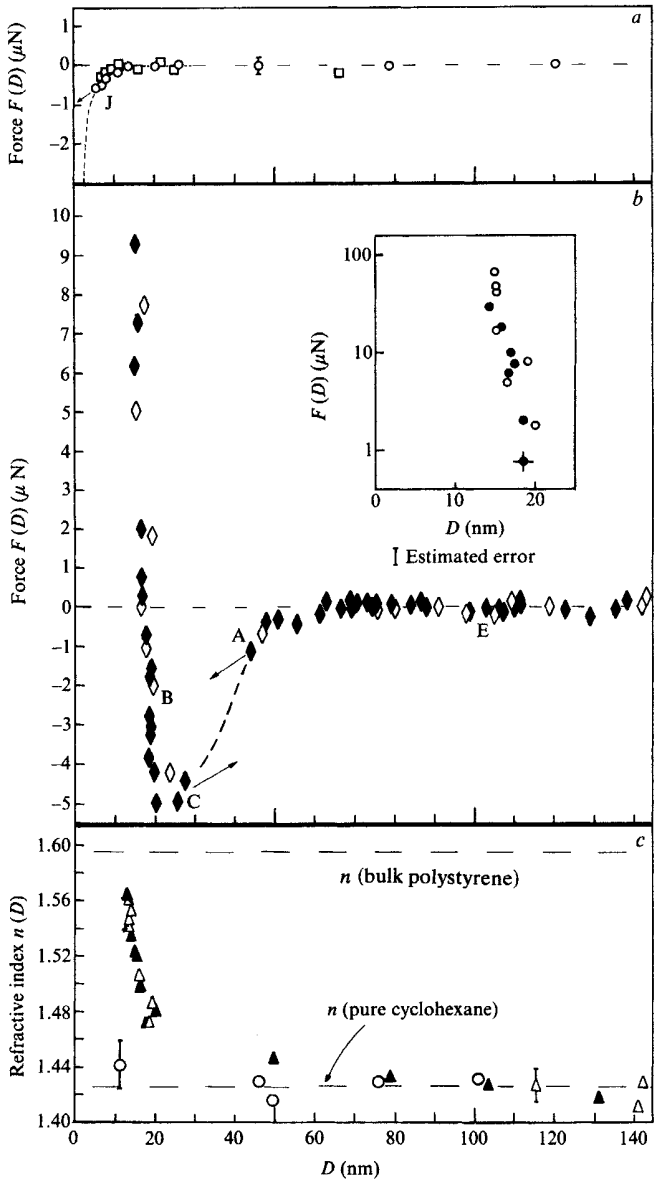

Fig. 2 Forces $F(D)$ and refractive index $n(D)$ between curved mica surfaces in cyclohexane (Fluka, spectroscopic grade) at 24.0 ± 0.5 °C. *a*, Forces between bare mica surfaces in pure cyclohexane. At J(7 ± 1 nm) the surfaces jump into contact within ±0.3 nm of their air contact position. Mica surfaces (where R is the mean radius of curvature of mica): □, $R = 0.35 \times 10^{-2}$ m; ○, $R = 0.66 \times 10^{-2}$ m. The broken line is the theoretical Van der Waals force $F(D) = -AR/6D^2$, with $R = 0.66 \times 10^{-2}$ m and a Hamaker constant $A = 1.4 \times 10^{-20}$ J, estimated from optical data for mica in cyclohexane *b*, Forces between the curved mica surfaces of *a* ($R = 0.66 \times 10^{-2}$ m) following 10 h incubation in a polystyrene cyclohexane solution. Solutions were prepared by overnight stirring of the polystyrene (Pressure Chemicals, $M_w = 5.99 \times 10^5$, $M_w/M_n \leq 1.06$) in cyclohexane, followed by 1-h ultracentrifugation at 160,000*g* before use. The inset extends the range of $F(D)$ on a semi-log plot. ◇, ○, Forces measured in the polymer solution; ◆, ●, forces following replacement of solution by pure solvent. At A, C the surfaces jump to new stable positions B, E (see text); AC (broken curve) is a region for which $\partial F/\partial D > K$ and $F(D)$ cannot be measured[8]. *c*, Refractive index $n(D)$, of the medium separating the mica surfaces. ○, in pure cyclohexane. △, in solution, following 10-h incubation. ▲, 20–44 h after replacing the polymer solution by pure solvent.

styrene (of similar molecular weight) adsorbed from cyclohexane onto various surfaces in θ conditions.

The initially attractive nature of the interactions, however, is to be expected: it arises because the polymer molecules adsorbed on each mica surface have a much greater affinity for those adsorbed on the opposing surface, than they do for the solvent molecules. As Flory has shown[5], bringing two polymer-segment distributions into overlap in worse than θ conditions (a negative second virial coefficient) results in a negative free energy change. Thus, on initial overlap, an attractive force arises between the surfaces; as they approach to much closer than a radius of gyration, the compression of the adsorbed layers by the mica surfaces leads to extensive configurational constraints on the polymer molecules[4], resulting in the ultimate strong repulsion observed at $D \leqslant 18$ nm.

Over the range of times and experimental parameters described, the present results indicate that: (1) in certain conditions the steric repulsion observed when two adsorbed polymer layers are mutually compressed is preceded by an attractive region; (2) the onset of steric interaction between the adsorbed layers may take place at surface separations comparable with the polymer dimensions and with layer thicknesses measured by other means; and (3) the polymer adsorption may be an irreversible process.

I thank Professor A. Silberberg for encouragement, interest and helpful discussions; also the design and workshop staff of the Weizmann Institute for technical assistance, and Dr J. N. Israelachvili for useful suggestions. This work was partly supported by the Basic Research Division of the Israel Academy of Sciences.

Received 17 June; accepted 12 September 1980.

1. Lyklema, H. & Van Vliet, T. *Faraday Discuss.* **65**, 25 (1978).
2. Cain, F. W., Ottewill, R. H. & Smitham, J. B. *Faraday Discus.* **65**, 33 (1978).
3. Israelachvili, J. N., Tandon, R. K. & White, L. R. *Nature* **277**, 120 (1979); *J. Coll. Interface Sci.* (in the press).
4. Vincent, B. *Adv. Coll. Sci.* **4**, 193 (1974).
5. Flory, P. J. *Principles of Polymer Chemistry* (Cornell University Press, Ithaca, 1953).
6. Tabor, D. & Winterton, R. H. S. *Proc. R. Soc.* **A312**, 435 (1969).
7. Israelachvili, J. N. & Tabor, D. *Proc. R. Soc.* **A331**, 19 (1972).
8. Israelachvili, J. N. & Adams, G. E. *JCS Faraday I* **74**, 975 (1978); *Nature* **262**, 774 (1976).
9. Stromberg, R. R., Tutas, D. J. & Passaglia, E. *J. phys. Chem.* **69**, 3955 (1965).
10. Schultz, A. R. & Flory, P. J. *J. Am. chem. Soc.* **74**, 4760 (1952).
11. Outer, P., Carr, C. I. & Zimm, B. H. *J. chem. Phys.* **18**, 830 (1950).
12. Rowland, F., Bulas, R., Rothstein, E. & Eirich, F. *Ind. Eng. Chem.* **57**, 49 (1965).
13. Brandrupp, J. & Immergut, E. H. (eds) *Polymer Handbook* 2nd edn (Wiley, New York, 1975).

Deep-seated iron ores from banded-iron formation

R. C. Morris, M. R. Thornber & W. E. Ewers

Division of Mineralogy, Institute of Earth Resources, CSIRO, Wembley, Western Australia 6014, Australia

Very large iron ore deposits have formed in many parts of the world, evidently by the supergene alteration of Precambrian banded-iron formation (BIF). Some of these deposits extend to great depths, ranging to 2,400 m at Krivoyrog[1], beyond the likely reach of oxygenated water. We propose here, on the basis of studies in the Hamersley Ranges, Western Australia, a mechanism for deep-seated ore formation in which electronic conduction through the magnetite layers in BIF connects a cathodic region near the surface, where oxygen is reduced, to an anode at depth, where iron (II) from magnetite, carbonates and silicates is oxidized and precipitated as iron (III) hydroxy-oxides. The electrical circuit is completed by ionic conduction through groundwaters. The model is based broadly on a mechanism suggested by Sato and Mooney[2] to explain self-potentials associted with sulphide ore bodies. It is based more specifically on a model demonstrated by Thornber[3] for the weathering of massive nickel–iron sulphide deposits at Kambalda, Western Australia, but with substantial differences in the physical situation and the reactions at depth.

The iron ore reserves of the Hamersley Iron Province exceed 33×10^9 tonnes, much of it contained in huge ore bodies, some of them exceeding 5 km along strike and extending below the present water table to as much as 400 m down dip. They conform to the bedding of the host BIF and, in common with many ore bodies of this kind throughout the world, grade from >60% Fe in ore to <30% Fe in BIF over distances that are always negligible in relation to the size of the ore body and sometimes much less than a metre.

BIF in the Hamersleys is characterized by compositional layering of the centimetre scale in mesobands, some of them magnetite-rich, alternating with others containing chert, haematite, magnetite, silicates and carbonates in varied proportions. Many of these mesobands can be traced individually for hundreds of kilometres[4].

Morris[5] has provided petrographical evidence that the Hamersley orebodies, in general, have formed from BIF by a combination of residual enrichment of the original iron oxides (magnetite, now martite, and primary haematite) by removal in solution of silica and other gangue, together with replacement of part of this gangue by hydrous iron oxide.

A key factor in the formation of ore at depth by such a process is the electrical conductivity of the magnetite-rich layers in BIF, and this may explain Dorr's[6] observation that ores "form best from the oxide facies iron-formation in most places of the world".

Table 1 lists some field and laboratory resisitivity measurements which indicate that BIF is highly conductive along the layers of magnetite. This conductivity is reatained even where the magnetite has been partially altered by weathering. Thus the BIF can be considered as an adequate conductor to allow higher oxidation potentials to penetrate to considerable depths as shown in Fig. 1*a*. The cathode, with a potentially vast area exposed along strike, comprises magnetite in contact with waters oxygenated by the atmosphere. Here electrons drawn from below would be consumed by the reduction of oxygen, summarized by the reaction:

$$O_2 + 2H_2O + 4e^- = 4OH^- \quad (1)$$

The reaction that can take place at anodic surfaces of magnetite at depth, remote from sources of atmospheric oxygen, is:

$$Fe^{2+} = Fe^{3+} + e^- \quad (2)$$

The supply of Fe^{2+} to the anode, mainly from the dissolution of iron (II) minerals, all of the carbonates and silicates, and some of the magnetite, is facilitated by the release of acid in the hydrolysis reaction which will occur close to the anode surface:

$$Fe^{3+} + 3H_2O = Fe(OH)_3 + 3H^+ \quad (3)$$

The chief apparent difficulty with this model is that galvanic processes would normally favour near-surface oxidation, that is, with the anode and cathode close together; for example, where an iron bar immersed in damp soil corrodes through near the soil–air interface. However, our experimental data, as well as field and mineragraphic observations, indicate that the

Table 1 Some resistivity measurements on banded-iron formation

Measured on	Resistivity (Ωm) Longitudinal ρ_e	Transverse ρ_t	Anisotropy coefficient $\lambda((\rho_t/\rho_e)^{1/2}$
Cliff face at Dales Gorge			
Mostly BIF	2.7	7,574	53
BIF + shale	4.5	7,800	42
Isolated slab 2 × 0.9 m thick	0.87	5.5×10^5	795
Rods 1-cm^2 cross-section			
Magnetite band	0.4	—	—
Chert-magnetite	740	8.6×10^5	34.2

0028–0836/80/470250—03$01.00